BJR

Received: 22 February 2016 | Revised: 11 June 2016 | Accepted: 27 June 2016

http://dx.doi.org/10.1259/bjr.20160173

Cite this article as:
Herek D, Karabulut A, Agladioglu K. Usefulness of transabdominal real-time sonoelastography in the evaluation of ovarian lesions: preliminary results. *Br J Radiol* 2016; **89**: 20160173.

FULL PAPER

Usefulness of transabdominal real-time sonoelastography in the evaluation of ovarian lesions: preliminary results

[1]DUYGU HEREK, MD, [2]AYSUN KARABULUT, MD and [1]KADIR AGLADIOGLU, MD

[1]Department of Radiology, School of Medicine, Pamukkale University, Denizli, Turkey
[2]Department of Gynecology and Obstetrics, School of Medicine, Pamukkale University, Denizli, Turkey

Address correspondence to: Dr Duygu Herek
E-mail: *dtherek@yahoo.com*

Objective: We aim to evaluate and describe the tissue elasticity characteristics of various ovarian lesions with sonoelastography.

Methods: 35 patients (age range 16–85 years; mean age 40.8 years) underwent sonoelastography and later MRI. Histopathological confirmation of all lesions was carried out, except eight of endometriomas and six of septated cysts which were confirmed on MRI and follow-up ultrasonography. Strain ratios and elastogram patterns were recorded. Lesions were classified into three groups (Group 1: cystic lesions, Group 2: benign tumours and Group 3: malignant lesions) and findings were compared between groups for both observers. Interobserver agreement was analyzed. Optimal cut-off values for strain ratios were achieved with receiver operating characteristic curve analysis.

Results: Ovarian endometriomas and complex cystic lesions were observed hard on elastograms with high strain ratios, and malignant lesions were observed mostly soft with very small strain ratios. Benign tumours had average tissue stiffness, observed harder than the malignant lesions, and strain ratios ranged from 4 to 14. The differences in patterns and strain ratios between groups were statistically significant ($p < 0.05$ for both observers).

Conclusion: Our study revealed that malignant ovarian lesions have softer tissue property than benign lesions and cystic lesions in terms of elastogram patterns and strain ratios.

Advances in knowledge: Most ovarian lesions contain solid and cystic parts which make the malignant and benign lesions look similar on imaging modalities. Using real-time sonoelastography as an adjunct to other imaging modalities may improve the differentiation of malignant ovarian lesions from benign lesions.

INTRODUCTION

Ovarian lesions have various imaging characteristics as being purely cystic, solid or cystic lesions with solid components.[1] Some cystic lesions are complex cysts with septations, haemorrhage or thick walls. Malignant lesions have different imaging characteristics as being pure solid or having solid and cystic components together. Differentiation between benign and malignant lesions is challenging in ovaries. First-line imaging tool is ultrasonography, either transabdominal or transvaginal.[1,2] According to the classification of the International Ovarian Tumour Analysis Group, solid lesions or multilocular cysts with solid component have the highest risk of malignancy.[2] Imaging with conventional greyscale ultrasonography, Doppler ultrasonography and/or MRI is important for diagnosis before deciding about surgery.[1] It is reported that subjective evaluation of greyscale ultrasonography characteristics, colour and power Doppler imaging and three-dimensional Doppler imaging characteristics of the ovarian malignant and benign lesions might differ, and each modality has some advantages over the other.[3,4] Benign and malignant masses of the ovary were proved to have vascularity but resistive index, pulsatility index or temporal average mean velocity measurements did not show specific changes in the differential diagnosis.[5] In a recent study, Doppler ultrasonography alone was shown to have a sensitivity of 71.88% and specificity of 84.28% in the identification of ovarian malignancies.[6] MRI is advantageous because it provides multiplanar imaging, high-contrast resolution and tissue differentiation. It is also important in characterization of biochemical states of blood and fat component that may exist in the lesions of ovaries.[7] Besides these advantages and its high spatial and contrast resolution, MRI has disadvantages of being more expensive than other modalities and requires longer imaging times. The need for contrast material usage that can end up with nephrogenic systemic fibrosis is another downside of MRI. Sonoelastography is a novel technique for assessing tissue stiffness which is recently being used for differentiation between malignant and benign lesions of the breast and thyroid.[8–11] We

thought that elastography property which is recently being adjusted to most of the high-quality ultrasonography scanners can also be used in the evaluation of ovarian masses. As shown in thyroid or breast lesions, elasticity characteristics of the ovarian lesions may also be used in the differentiation of malignant and benign lesions. Because almost all patients with pelvic complaints undergo ultrasonography examinations, use of elastography is easy by just switching the scanner into elastography mode. We thought that if any elastographic pattern characteristics could be established, it would be a cost-effective approach to the management of patients with ovarian lesions by preventing most of the patients from undergoing unnecessary MRI, and it would add much more information to the greyscale and colour Doppler ultrasonography evaluation of the lesions. Therefore in this study, we aimed to evaluate various ovarian lesions with real-time strain elastography (RTSE) and tried to describe the tissue elasticity characteristics of malignant and benign ovarian masses. To the best of our knowledge, there is no study in the literature which evaluates the tissue elasticity of different ovarian masses with sonoelastography.

METHODS AND MATERIALS

Study population, equipment and scanning

This study was approved by the local ethics committee. 33 patients (age range 16–85 years; mean age 40.8 years) were enrolled consecutively in this study. All patients presented with right or left lower quadrant pain, pelvic fullness, vaginal discharge or menstrual irregularities. Written informed consent was obtained before the examinations. Patients who were overweight and obese were excluded from the study because effective compression to create a colour-coded map of the mass was not possible in these patients. Also, patients who had small follicular cysts or simple dominant follicles in the ovaries or diagnosed with polycystic ovarian syndrome and did not undergo MRI were excluded from the study. Patients with complex ovarian masses to which effective compression was available by transabdominal sonographic approach were included in this study. The final diagnoses were endometrioma ($n = 10$), septated complex cyst ($n = 4$), dermoid cyst ($n = 3$), mature cystic teratoma ($n = 2$), immature teratoma ($n = 1$), mucinous cystadenoma ($n = 2$), sclerosing stromal tumour (SST) ($n = 2$), Krukenberg tumour ($n = 1$), granulocytic sarcoma ($n = 1$), Brenner tumour ($n = 2$), high-grade serous adenocarcinoma ($n = 5$).

Dermoid cysts, teratomas, Krukenberg tumour, granulocytic sarcoma, Brenner tumours, SSTs, mucinous cystadenomas, high-grade serous adenocarcinomas, six of the endometriomas and one of the complex cyst were confirmed by means of histopathological examination. The rest of the endometriomas and cysts were confirmed by their imaging characteristics on MRI and monthly follow-up ultrasonography.

All patients included in the study underwent pelvic MRI that was performed with a 1.5-T superconducting system (Signa™ Excite; GE Healthcare, Milwaukee, WI) using an eight-channel phased-array torso coil. Axial T_1 weighted three-dimensional spoiled gradient echo pulse sequence with fat suppression before and after gadolinium-based contrast material injection was obtained. Also, axial T_1 weighted gradient echo sequence without fat suppression and axial and coronal T_2 weighted fast spin echo sequences were obtained. Subtraction MRI was also obtained.

Patients underwent transabdominal sonoelastographic examination with a sonographic scanner (LOGIQ™ E9; GE Healthcare) with an elastography-compatible 1- to 5-MHz convex probe. None of the patients had transvaginal sonographic evaluation because a transvaginal transducer was not available. Two different radiologists with 10 years' experience in conventional ultrasonography and 3 years' experience in sonoelastography who were blinded to each other's measurements did the examinations separately. They also did not know the histopathology or the diagnosis on MRI. First conventional transabdominal ultrasonography was performed and ovarian lesions were located. Then, the scanner was switched into elastographic mode. Greyscale sonogram and elastogram images were displayed simultaneously in the dual mode. Local strain was achieved by freehand technique with vertical compressions–decompressions.[12,13] The quality of compression was indicated on a scale between 1 and 7 using a quality feedback bar. At least five bars of the indicator should be active for optimal compression. Tissue stiffness was displayed on a colour-coded map where red areas indicate soft-tissue parts, green areas indicate intermediate and blue areas indicate hard-tissue parts.

Image analysis

All static images were recorded and stored in the local sonography device for later review. Sonoelastograms were classified into five colour-overlay patterns according to tissue hardness explained by different authors in the literature.[8,14,15] Colour mapping was set as blue being the hardest and red being the softest tissue parts. The five colour-overlay patterns were as follows: Pattern 1: an absent or a very small hard area with mostly soft-tissue parts seen as red and green, Pattern 2: green areas representing intermediate tissue stiffness with hard-tissue (blue) parts appearing less than 50%, Pattern 3: intermediate tissue stiffness with hard-tissue parts appearing more than 50%, Pattern 4: peripheral hard-tissue and central soft-tissue parts, Pattern 5: lesion is entirely hard with blue areas appearing more than 90%. Strain ratios for all the lesions were calculated. The first region of interest (ROI) was placed on a reference tissue part. Selection of the reference area is important in strain ratio calculations. Therefore, we chose the softest area coded as red (E1) neighbouring the lesion for standardized calculations. The second ROI was placed on the lesion including the entire lesion area (E2). Placement of ROIs was performed by the radiologists during the examination of patients with sonoelastography. Strain ratio (E2/E1) was automatically calculated by the scanner.

After sonoelastography, all patients underwent MRI. All MR images were reviewed by one of the radiologist with 7 years' experience in abdominal MRI. Endometrioma diagnosis was carried out by specific characteristics such as hyperintense lesion on unenhanced fat-saturated T_1 weighted images, no enhancement on T_1 weighted subtraction images and T_2 shading on T_2 weighted images seen as loss of signal intensity including, especially, the

Table 1. Distribution of strain ratios and elastogram patterns according to ovarian lesions for both observers

Diagnosis	Strain ratio		Elastogram pattern	
	Observer 1	Observer 2	Observer 1	Observer 2
Endometrioma ($n = 10$)	9.53 ± 0.60	9.24 ± 0.60	4.5 ± 0.17	4.6 ± 0.22
Septated cysts ($n = 4$)	10.4 ± 2.30	10.3 ± 2.34	4.28 ± 0.28	4.14 ± 0.34
Dermoid cyst ($n = 3$)	4 ± 1.74	3.8 ± 1.74	2.33 ± 1.15	2.33 ± 1.15
Sclerosing stromal tumour ($n = 2$)	5.4 ± 0.55	5.3 ± 0.57	2.5 ± 0.5	3 ± 0.00
Mucinous cystadenoma ($n = 2$)	14.7 ± 4.7	14.7 ± 4.3	4 ± 1.00	4 ± 1.00
Brenner tumour ($n = 2$)	9.4 ± 0.35	9.4 ± 0.55	4 ± 0.00	4.5 ± 0.50
Mature cystic teratoma ($n = 2$)	11.8 ± 4.8	12.1 ± 4.9	4.5 ± 0.50	4.5 ± 0.50
Immature teratoma ($n = 1$)	5.8	5	3	3
Krukenberg tumour ($n = 1$)	1.27	1.17	1	1
Granulocytic sarcoma ($n = 1$)	1.5	1.3	2	1
High-grade serous adenocarcinoma ($n = 5$)	1.32 ± 0.65	1.28 ± 0.57	1.47 ± 1.15	1.8 ± 1.35

n, number of lesions.
Data presented as ± standard error of mean.

dependent layer of the cystic lesion. Complex septated cysts were cystic lesions with septations and/or thick walls without gadolinium enhancement on T_1 weighted contrast-enhanced series.

Statistical analysis

The SPSS® v. 17.0 for Windows® software package (IBM Corp., New York, NY; formerly SPSS Inc., Chicago, IL) was used for statistical data analysis. Data are presented as the mean ± standard error of mean. Differences between variables were assessed by Kruskal Wallis and Mann–Whitney *U* tests. A *p*-value of 0.05 or less was defined as significant. Diagnostic performance of RTSE for each radiologist based on strain ratios was also calculated using receiver operating characteristic (ROC) curve analysis. The area under the ROC curve was categorized as follows: <0.60: worthless, 0.61–0.70: poor, 0.71–0.80: fair, 0.81–0.90: good and 0.91–1.00: excellent. The elastogram patterns were compared between the radiologists using the weighted Cohen's kappa coefficient (κ). Intraclass correlation coefficient with confidence interval of 95% was used to assess the concordance between the radiologists in terms of strain ratio measurements. Interobserver agreement was categorized as follows: 0–0.20, poor; 0.21–0.40, fair; 0.41–0.60, moderate; 0.61–0.80, substantial; and 0.81–1.00, almost perfect.[16]

RESULTS

Mean strain ratio values and patterns of the lesions for both observers were given in Table 1. According to the calculations, cystic lesions were mostly Patterns 3, 4 and 5 showing hard-tissue property. Malignant lesions were soft with Patterns 1 and 2, and strain ratios ranged between 1 and 4. Benign lesions with solid and cystic parts (benign ovarian tumours) had different tissue elasticity with cystic parts observed harder than their solid component. Mostly Patterns 3 and 4 were observed, and strain ratios ranged from 4 to 14 in these benign tumours. We also classified the lesions into three groups as: Group 1 being benign and entirely cystic without any solid components, Group 2 being benign but having solid parts (pathologically proven benign ovarian tumours) and Group 3 proven to be malignant by histopathological examination. Group 1 ($n = 14$) consisted of septated cysts and endometriomas; Group 2 ($n = 11$) consisted of dermoids, mucinous cystadenomas, Brenner tumours, SSTs and mature cystic teratoma; and Group 3 ($n = 8$) consisted of high-grade serous adenocarcinomas, immature teratoma,

Table 2. Comparison of mean strain ratios and elastogram patterns between groups for both observers

Groups	Strain ratios		Elastogram patterns	
	Observer 1	Observer 2	Observer 1	Observer 2
Group 1 ($n = 14$)	9.8 ± 0.84	9.59 ± 0.84	4.4 ± 0.19	4.4 ± 0.14
Group 2 ($n = 11$)	8.6 ± 1.59[a]	8.6 ± 1.65[a]	3.3 ± 0.36[a]	3.5 ± 0.36[a]
Group 3 ($n = 8$)	2.48 ± 0.65[a,b]	2.2 ± 0.55[a,b]	1.86 ± 1.1[a,b]	1.70 ± 1.3[a,b]

n, number of lesions.
Data presented as ± standard error of mean.
[a]$p < 0.05$ compared with Group 1.
[b]$p < 0.05$ compared with Group 2.

Figure 1. Greyscale (a) and elastogram (b) images of a serous adenocarcinoma (white arrows) in the right ovary of a 58-year-old female show Pattern 1. Placement of regions of interest is shown (c).

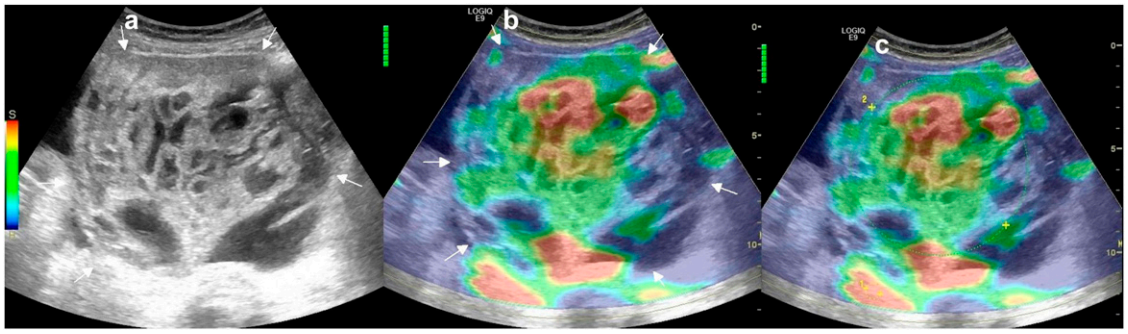

granulocytic sarcoma and Krukenberg tumour. The mean of the greatest diameters (mean ± standard error of mean) of the lesions according to groups were 8.5 ± 1 cm (range between 2.3 and 15 cm) for Group 1, 6.8 ± 0.83 cm (range between 2.5 and 11.5 cm) for Group 2 and 9.5 ± 1.4 cm (range between 5 and 15 cm) for Group 3. There was statistically significant difference in strain ratios and patterns between Groups 1 and 3 for both observers (strain ratios: $p = 0.01$ and 0.008 for Observers 1 and 2, respectively, and elastogram patterns: $p = 0.004$ for both observers). The findings between Groups 1 and 2 were statistically significant for elastogram patterns and strain ratios for both observers (elastogram patterns: $p = 0.010$ and 0.028 for Observers 1 and 2, respectively, and strain ratios: $p = 0.004$ and 0.01 for Observers 1 and 2, respectively). Difference in strain ratios and elastogram patterns were also statistically significant between Groups 2 and 3 (strain ratios: p-value of 0.047 for Observer 1 and 0.046 for Observer 2, respectively, and elastogram patterns: $p = 0.043$ and 0.041 for

Figure 2. A 43-year-old female with histopathologically proven Brenner tumour (white arrows) in her left adnexal region. Greyscale (a) and elastogram (b) show Pattern 4. After placement of the regions of interest (c, d), automatically derived strain ratio (E2/E1) is 9.4.

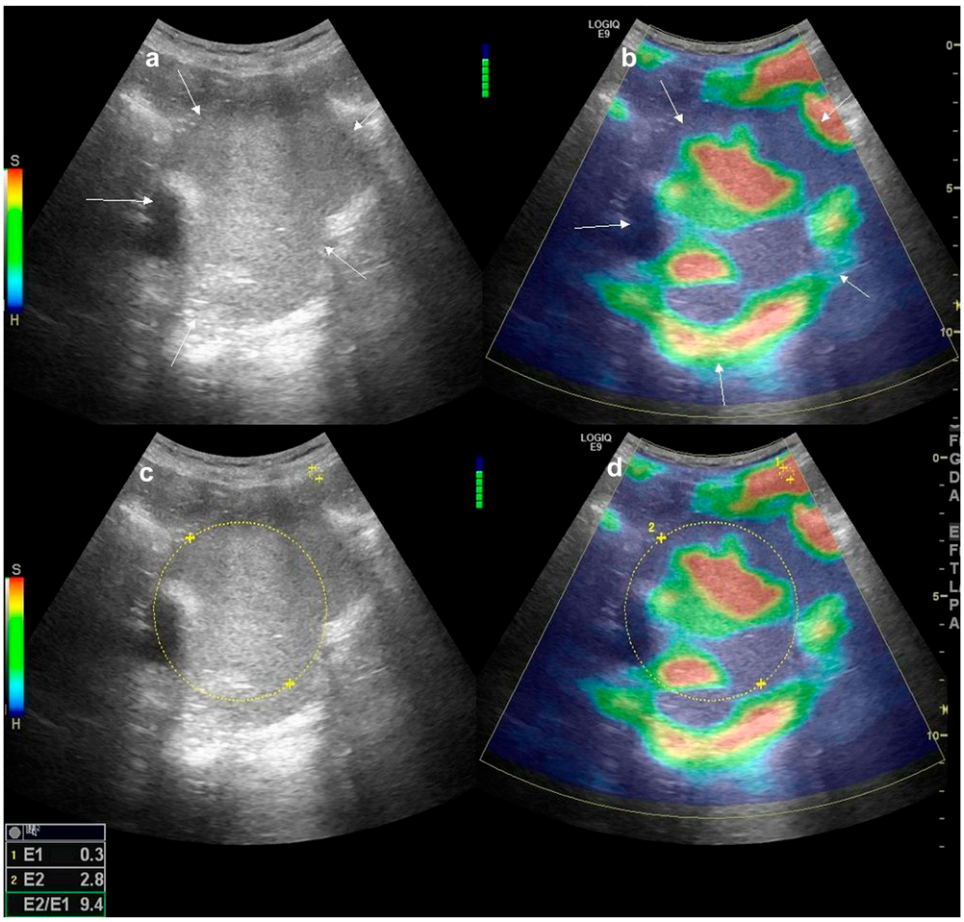

Figure 3. Greyscale (a) and elastogram (b) images of a 29-year-old female show a complex ovarian cyst (white arrows) with thick wall. Pattern 3 is observed on elastogram (b, d). Automatically derived strain ratio (E2/E1) is 8.3 (c, d).

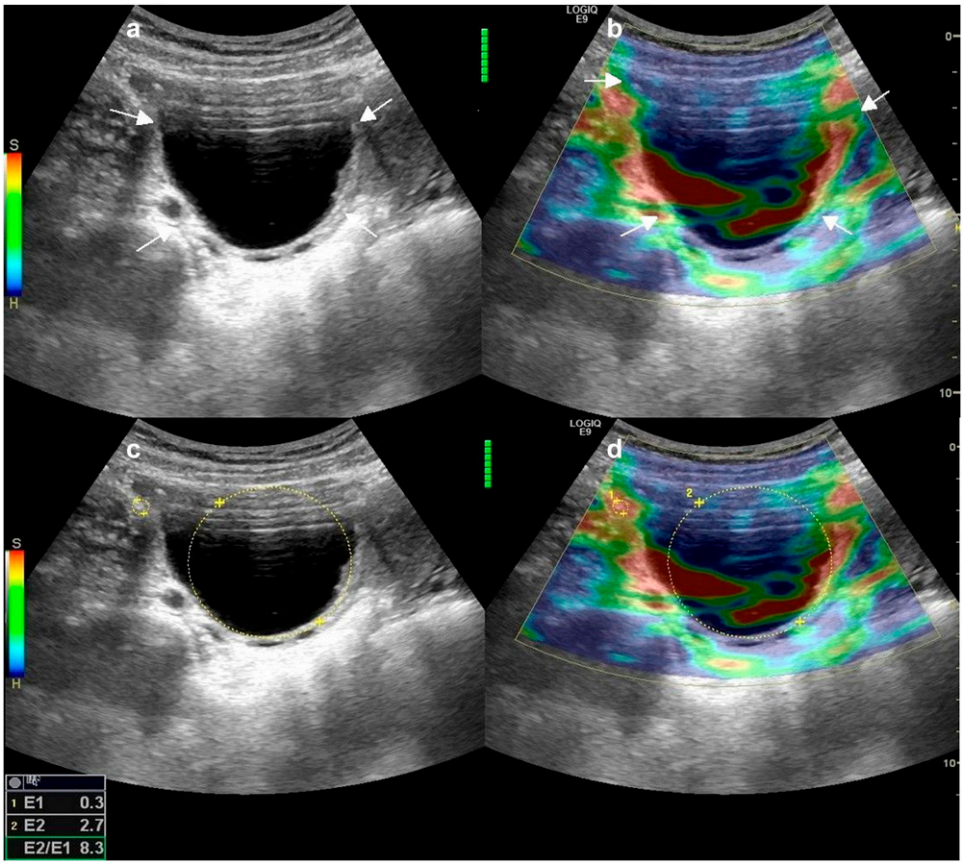

Observers 1 and 2, respectively). The findings among Groups 1, 2 and 3 are given in Table 2. Figures 1–4 provide examples of different elastogram patterns of various ovarian lesions.

The concordance between the radiologists was substantial (κ: 0.73, $p < 0.001$) for elastogram patterns and was excellent (intraclass correlation coefficient: 0.97, $p < 0.001$) for strain ratios for all ovarian lesions.

The ability of RTSE to differentiate between lesions was quantified by ROC curve analysis. Area under the curve for differentiation of complex cystic lesions (Group 1) from malignant lesions (Group 3); benign tumours (Group 2) from malignant tumours (Group 3); and benign tumours (Group 2) from complex cystic lesions (Group 1) based on strain ratios was calculated for each observer. Table 3 gives the optimal cut-off values for strain ratios, and sensitivity and specificity values for both observers.

DISCUSSION

This study reveals that unlike malignant lesions of other organs such as the thyroid and breast which were reported as having hard-tissue property on elastograms, tissue elasticity of ovarian malignant lesions tends to be softer.[17,18] The difference in tissue elasticity is clearly observed between entirely cystic lesions and solid malignant lesions. Benign tumours with solid and cystic parts mostly showed intermediate tissue elasticity, especially average tissue stiffness in their solid parts and increased tissue stiffness seen as blue in their cystic parts on elastograms. The elasticity differences in terms of pattern and strain ratio were also statistically significant between benign and malignant tumours (Groups 2 and 3).

Recently in a study carried out with transabdominal real-time sonoelastography in high- and low-grade serous ovarian cancers, high-grade lesions were found to be less stiff.[14] This property was reported to may be related with the necrosis within the tumours. In our study, although serous carcinomas, granulocytic sarcoma and Krukenberg tumour were pathologically reported to have also necrosis, immature teratoma pathologically had different immature and mature tissue parts with mucous glandular structures but not necrosis. This pathological difference was also reflected in the values of strain ratios and elastogram patterns. Immature teratoma was pathologically grade 2 which had strain ratios of 5.8 and 5 and Pattern 3 for both observers on elastography. On the contrary, serous carcinomas, Krukenberg tumour and granulocytic sarcoma had very low strain ratios with elastogram patterns assigned as 1 and 2 (Table 1). Therefore, these findings also showed us that necrosis might be the reason that malignant lesions of the ovary had softer tissue property on elastograms. Also, another study which was performed with sonoelastography investigated the response of high-

Figure 4. Greyscale (a) and elastogram (b) images of a 28-year-old female with endometrioma (white arrows) in her left ovary show Pattern 5. After placement of regions of interest (c, d), automatically derived strain ratio (E2/E1) is 12.2. It was hyperintense on unenhanced T_1 weighted images, and no enhancement was seen on subtraction series on MRI.

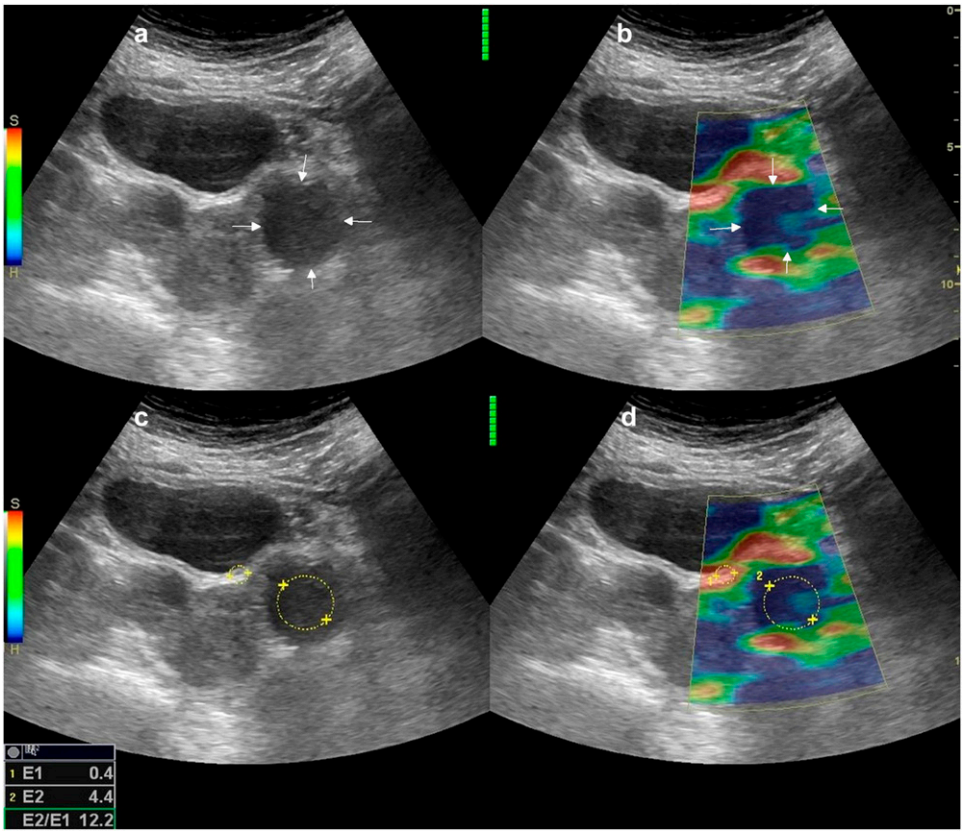

grade serous ovarian cancer to neoadjuvant chemotherapy revealed that tumour got stiffer after the treatment.[19] This also shows that malignant ovarian lesions are soft on elastogram but tissue stiffness increases after tumour treatment. Hence, benignity and/or response to treatment in an ovarian lesion is presented as hard elastogram pattern and increased strain index.

According to our study benign ovarian tumours seem to have higher stiffness than malignant lesions. Strain ratios of SSTs were calculated as 5.3 and 5.4 for both observers with patterns representing average tissue stiffness, whereas Brenner tumours had a strain ratio of 9.4, showing harder elastograms than SSTs (Table 1). The differences in strain ratios and elastograms between benign and malignant tumours were significant, and benign tumours have harder tissue property than malignant lesions. Onur et al[20] reported that SST of an ovary had similar tissue stiffness as the myometrium that demonstrated high stromal component in the tumour. We also think that as the stromal component increases, tissue stiffness increases on elastography in an ovarian tumour. In a study with females who had polycystic ovarian syndrome, elastography revealed higher strain ratios than that of the control group.[15] They thought that this change was also because of the hard stroma within the ovaries affected by the disease. In the light of present knowledge, we think that necrosis in an ovarian lesion causes low tissue elasticity and more stromal component causes increased tissue stiffness.

In our study, both radiologists calculated almost similar strain ratios for the lesions in all groups with an excellent concordance.

Table 3. Receiver operating characteristic curve analysis with optimal cut-off values to differentiate lesions between groups based on strain ratios

Parameter	Radiologist 1			Radiologist 2		
	Groups 1–2	Groups 1–3	Groups 2–3	Groups 1–2	Groups 1–3	Groups 2–3
Optimal cut-off (strain ratio)	7.9	6.5	5.3	7.7	6.5	5.2
Area under the curve	0.62	0.98	0.89	0.61	0.98	0.88
Sensitivity (%)	64	86	70	62	86	70
Specificity (%)	55	100	87	55	100	92

Therefore, based on this fact, we tried to compare diagnostic performance of RTSE in the evaluation of ovarian lesions by using optimal cut-off value for strain ratios between each of the three groups. According to our findings, complex cysts and benign ovarian tumours may not be effectively distinguished from each other by using strain ratios but malignant tumours from benign tumours and complex cystic lesions can be efficiently discriminated by using RTSE. Complex cysts of the ovary contain septations, thick walls and sometimes haemorrhage and mural nodules, and endometriomas also contain blood products both of which are seen as complex lesions on ultrasonography. Endometriomas are even seen as solid lesions on ultrasonography because they are protean in their sonographic appearances and overlap in imaging features of complex cystic lesions, and benign and/or malignant lesions make these lesions difficult to be distinguished from each other.[21] Strain ratios and elastogram patterns of the cystic lesions were observed to be similar to benign tumours on RTSE in the current study, and RTSE seemed to be ineffective in discriminating the lesions of Group 1 from the lesions in Group 2 according to the ROC analysis.

In different studies, determinant of tissue stiffness in cystic lesions was reported to be caused by the fluid content itself.[18,22] In simple breast cysts, an aliasing artefact as blue–green–red (BGR) pattern was reported on elastography.[23] In our study, cystic lesions were not simple cysts; instead, they were mostly endometriomas and septated cysts but did not contain solid component. They had Patterns 4 and 5 on elastograms with very high strain ratios representing hard-tissue property. Fluid content in an ovarian lesion appeared blue, representing increased stiffness on elastograms in the current study. This showed us that RTSE can be used as a promising tool in the differentiation of cystic ovarian lesions from solid lesions where cysts would have high tissue stiffness, appearing blue as observed in this study. Studies with elastography in breast lesions already reported that cysts had no elasticity appearing black or entirely blue.[24] According to our results, this characteristic also applies to ovarian lesions where cysts and cystic component of the lesions will appear hard. Sonoelastography is also reported to be used for the obviation of some unnecessary diagnostic biopsies in cystic lesions of the breast.[14,25] We also think that RTSE could prevent unnecessary MRI for ovarian lesions by differentiating simple or complex cystic lesions from solid masses.

This study had some limitations. The first and main limitation is that our sample population was small, but the number of patients in all groups was at least close to each other. Second, we had to use a scoring system adapted from different studies because of the lack of a widely accepted scoring criteria for elastograms in ovarian lesions. We hope our study can be a guide for further ovarian sonoelastography studies. Third, not all the endometriomas and septated cysts had histopathological confirmation, but they are radiologically well recognized on MRI and follow-up ultrasonography; therefore, we think that this limitation can be ignored. Lastly, because of our technical handicap, that is, because a transvaginal transducer was not available on our scanner, we could not obtain transvaginal evaluations of the lesions.

In conclusion, this study establishes that malignant lesions of ovaries have soft-tissue characteristics on elastograms with very low strain ratios. However, cystic lesions as endometriomas, complex cysts or cystic parts of other lesions possess increased tissue stiffness on elastograms. Benign tumours also have harder tissue elasticity than malignant lesions. These results suggest that RTSE can be an adjunct to other imaging methods in the differentiation of malignant and benign ovarian lesions and might reduce the costs resulting from unnecessary MRIs. As far as we know, our study is the first RTSE study that included various ovarian lesions, but more clinical observation and research with sonoelastography should be conducted to prove the validity of these findings.

REFERENCES

1. Choi JI, Park SB, Han BH, Kim YH, Lee YH, Park HJ, et al. Imaging features of complex solid and multicystic ovarian lesions: proposed algorithm for differential diagnosis. *Clin Imaging* 2016; **40**: 46–56. doi: http://dx.doi.org/10.1016/j.clinimag.2015.06.008
2. Dias DS, Bueloni-Dias FN, Delmanto A, Tonon AF, Tayfour NM, Traiman P, et al. Clinical management of incidental findings on pelvic adnexal masses. *Rev Assoc Med Bras* 2015; **61**: 469–73. doi: http://dx.doi.org/10.1590/1806-9282.61.05.469
3. Jokubkiene L, Sladkevicius P, Valentin L. Does three-dimensional power Doppler ultrasound help in discrimination between benign and malignant ovarian masses? *Ultrasound Obstet Gynecol* 2007; **29**: 215–25. doi: http://dx.doi.org/10.1002/uog.3922
4. Guerriero S, Ajossa S, Risalvato A, Lai MP, Mais V, Angiolucci M, et al. Diagnosis of adnexal malignancies by using color Doppler energy imaging as a secondary test in persistent masses. *Ultrasound Obstet Gynecol* 1998; **11**: 277–82. doi: http://dx.doi.org/10.1046/j.1469-0705.1998.11040277.x
5. Tailor A, Jurkovic D, Bourne TH, Collins WP, Campbell S. Sonographic prediction of malignancy in adnexal masses using multivariate logistic regression analysis. *Ultrasound Obstet Gynecol* 1997; **10**: 41–7. doi: http://dx.doi.org/10.1046/j.1469-0705.1997.10010041.x
6. Zhang F, Zhang ZL. The diagnostic value of transvaginal sonograph (TVS), color Doppler, and serum tumor marker CA125, CEA, and AFP in ovarian cancer. *Cell Biochem Biophys* 2015; **72**: 353–7. doi: http://dx.doi.org/10.1007/s12013-014-0463-x
7. Foti PV, Attinà G, Spadola S, Caltabiano R, Farina R, Palmucci S, et al. MR imaging of ovarian masses: classification and differential diagnosis. *Insights Imaging* 2016; **7**: 21–41. doi: http://dx.doi.org/10.1007/s13244-015-0455-4
8. Gweon HM, Youk JH, Son EJ, Kim JA. Clinical application of qualitative assessment for breast masses in shear-wave elastography. *Eur J Radiol* 2013; **82**: e680–5. doi: http://dx.doi.org/10.1016/j.ejrad.2013.08.004
9. Yoon JH, Ko KH, Jung HK, Lee JT. Qualitative pattern classification of shear wave elastography for breast masses: how it correlates to quantitative measurements. *Eur J Radiol* 2013; **82**: 2199–204. doi: http://dx.doi.org/10.1016/j.ejrad.2013.08.047

10. Lacout A, Chevenet C, Thariat J, Figl A, Marcy PY. Qualitative ultrasound elastography assessment of benign thyroid nodules: patterns and intra-observer acquisition variability. *Indian J Radiol Imaging* 2013; **23**: 337–41. doi: http://dx.doi.org/10.4103/0971-3026.125612
11. Itoh A, Ueno E, Tohno E, Kamma H, Takahashi H, Shiina T, et al. Breast disease: clinical application of US elastography for diagnosis. *Radiology* 2006; **239**: 341–50. doi: http://dx.doi.org/10.1148/radiol.2391041676
12. Ophir J, Alam SK, Garra B, Kallel F, Konofagou E, Krouskop T, et al. Elastography: ultrasonic estimation and imaging of the elastic properties of tissues. *Proc Inst Mech Eng H* 1999; **213**: 203–33. doi: http://dx.doi.org/10.1243/0954411991534933
13. Doyley MM, Bamber JC, Fuechsel F, Bush NL. A freehand elastographic imaging approach for clinical breast imaging: system development and performance evaluation. *Ultrasound Med Biol* 2001; **27**: 1347–57. doi: http://dx.doi.org/10.1016/S0301-5629(01)00429-X
14. Xie M, Zhang X, Zhan J, Hua K. Application of real-time ultrasound elastography for discrimination of low- and high-grade serous ovarian carcinoma. *J Ultrasound Med* 2013; **32**: 257–62.
15. Çıracı S, Tan S, Özcan AŞ, Aslan A, Keskin HL, Ateş ÖF, et al. Contribution of real-time elastography in diagnosis of polycystic ovary syndrome. *Diagn Interv Radiol* 2015; **21**: 118–22.
16. Landis JR, Koch GG. The measurement of observer agreement for categorical data. *Biometrics* 1977; **33**: 159–74. doi: http://dx.doi.org/10.2307/2529310
17. Moon HJ, Sung JM, Kim EK, Yoon JH, Youk JH, Kwak JY. Diagnostic performance of gray-scale US and elastography in solid thyroid nodules. *Radiology* 2012; **262**: 1002–13. doi: http://dx.doi.org/10.1148/radiol.11110839
18. Rago T, Vitti P. Role of thyroid ultrasound in the diagnostic evaluation of thyroid nodules. *Best Pract Res Clin Endocrinol Metab* 2008; **22**: 913–28. doi: http://dx.doi.org/10.1016/j.beem.2008.09.016
19. Xie M, Zhang X, Jia Z, Ren Y, Wang W. Elastography, a sensitive tool for the evaluation of neoadjuvant chemotherapy in patients with high-grade serous ovarian carcinoma. *Oncol Lett* 2014; **8**: 1652–6. doi: http://dx.doi.org/10.3892/ol.2014.2346
20. Onur MR, Simsek BC, Kazez A. Sclerosing stromal tumor ovary ultrasound elastography MRI findings preoperative diagnosis. *J Med Ultrason* 2011; **38**: 217–20. doi: http://dx.doi.org/10.1007/s10396-011-0311-1
21. Lee SI. Radiological reasoning: imaging characterization bilateral adnexal masses. *AJR Am J Roentgenol* 2006; **187**: S460–6. doi: http://dx.doi.org/10.2214/AJR.05.2226
22. Bhargava S, Bhargava SK, Sharma S, Prakash M. Elastography: a new imaging technique and its application. *JIMSA* 2013; **26**: 25–30.
23. Chiorean A, Duma MM, Dudea SM, Iancu A, Dumitriu D, Roman R, et al. Real-time ultrasound elastography of the breast: state of the art. *Med Ultrason* 2008; **10**: 73–82.
24. Iame.com (homepage on the internet). Institute for advanced medical education, online courses, breast elastography (date of release and review: 28 November, 2012 and 16 June, 2015). Available from: https://iame.com/online/breast_elastography/content.php
25. Garra BS. Elastography: current status, future prospects, and making it work for you. *Ultrasound Q* 2011; **27**: 177–86. doi: http://dx.doi.org/10.1097/RUQ.0b013e31822a2138